# TU3E-6

Accepted to the IEEE MTT-S Microwave Conference 2000

# CHARACTERIZATION OF MICROMACHINED TRANSMISSION LINES USING MRTD (MULTIRESOLUTION TIME DOMAIN TECHNIQUE)

Nathan Bushyager, Manos M. Tentzeris
(etentze@ece.gatech.edu)
School of ECE, Georgia Institute of Technology, Atlanta, GA 30332–250, U.S.A.

**Abstract-** The Haar-based MRTD algorithm is extended to 2.5D and is applied to the characterization of micromachined transmission lines. Simulation results of $\epsilon_{eff}$ for Si-micromachined Finite-Ground Coplanar Waveguides (FG-CPW) as a function of the undercut and for frequencies between 10 GHz and 60 GHz are compared to those obtained by use of conventional FDTD to indicate considerable savings in memory and computational time and demonstrate the adaptive modeling of multidielectric cells.

## I Introduction

Significant attention is being devoted now-a-days to the modeling of various types of micromachined devices that improve significantly the RF characteristics of waveguiding and radiating geometries (e.g. Low-loss performance, easy design and fabrication) used in Wireless and High-speed Computing applications. Though the Finite-Difference Time-Domain (FDTD) technique is one of the most popular time-domain design tools, the Battle-Lemarie based Multiresolution Time-Domain (MRTD) technique has been successfully applied [1] [3] to a variety of microwave problems and has demonstrated significant savings in memory and execution time requirements by one and two orders of magnitude respectively. The finite-domain Haar basis functions (Fig.(1)) provide a convenient tool for the transition from FDTD to MRTD due to their compact support, and to their similarity with the FDTD pulse basis [4]–[6], thus alleviating the problems due to the entire-domain nature of Battle-Lemarie expansion basis. Since the stability limit of the time-step decreases as more resolutions are added, the use of an effective multi-time-stepping algorithm, that will maintain the required accuracy without increasing significantly the execution time requirements, is necessary. In addition, the modeling of nonorthogonal dielectric interfaces has to be performed with minimal computational overhead. In this paper, a 2.5D extension of this MRTD scheme is used to model the propagation characteristics of Si-micromachined FG-CPW's. As an example, $\epsilon_{eff}$ is calculated as a function of the percentage of the dielectric undercut for a wide frequency range and results are compared with those obtained with FDTD.

## II The MRTD scheme

To derive the MRTD scheme, the field components are expanded in a series of Haar scaling and wavelet functions in space and pulse functions in time. The MRTD equations are derived by applying the Method of Moments to the Maxwell's equations after inserting the field expansions. For simplicity, the 1D MRTD scheme for TEM ($E_x$,$H_y$) propagation will be discussed. It can be extended to 2D, 2.5D and 3D in a straightforward way. The Electric ($E_x$) and the Magnetic ($H_y$) fields are displaced by half step in both time- and space-domains (Yee cell formulation) and are expanded in a summation of scaling ($\phi$) and wavelet ($\psi_r$) functions in space and scaling components in time. For example, $E_x$ is given by

$$E_x(z,t) = \sum_{m,i=-\infty}^{\infty} \left( {}_mE^{\phi}_{x,i}\phi_i(z) + \sum_{r=0}^{r_{max}} \sum_{i_r=1}^{2^r} {}_mE^{\psi_{r,i_r}}_{x,i}\psi_i^{r,i_r}(z) \right) \phi_m(t) \quad (1)$$



 

where $\phi_i(z) = \phi(z/\Delta z - i)$ and $\psi_i^{r,i_r}(z) = 2^{r/2}\psi_0(2^r(z/\Delta z - i_r) - i)$ represent the Haar scaling and r-resolution wavelet functions located inside the $i-$cell. The conventional notation ${}_mE_{x,i}$ is used for the voltage component at time $t = m\Delta t$ and $z = i\Delta z$, where $\Delta t$ and $\Delta z$ are the time-step and the spatial cell size respectively. The notation for $H_y$ is similar. Substituting $E_x$,$H_y$ in the TEM equations and applying Galerkin technique derives the following equations for $H_y$ scaling coefficients

$$
\begin{aligned}
{}_{m+0.5}H^{\phi}_{y,i-0.5} &= {}_{m-0.5}H^{\phi}_{y,i-0.5} - \frac{\Delta t}{\mu \Delta z} \left({}_mE^{\phi}_{x,i} + \right. \\
&+ \sum_{r=1}^{r_{max}} (c^{2^r,-1}_{1,r}\, {}_mE^{\psi_r,2^r}_{x,i-1} + c^{1,1}_{1,r}\, E^{\psi_r,1}_{x,i+1} \\
&+ \left. \sum_{i_{r1}=1}^{2^{r_{max}}} c^{i_{r1},0}_{1,r}\, {}_mE^{\psi_r,i_r}_{x,i}) - E^{\phi}_{x,i-1} \right) \quad (2)
\end{aligned}
$$

where the $c$ coefficients can be calculated correlating the respective wavelet and scaling functions. Since the wavelet coefficients have significant values only close to discontinuities or in areas of fast field variation, a combination of a relative and an absolute thresholds can be used for the identification of the higher needed resolution per cell. Usually, only wavelet terms with values absolutely larger than $10^{-6}$ and than $10^{-4}$ of the respective scaling coefficient are maintained and offer accuracy better than 0.1% and memory economy by a factor of 2-8 per dimension.

Since the grid position of a Perfect Electric Conductor (P.E.C.) can be chosen so as to coincide with the midpoint of the domain of the tangential Electric field scaling function, i.e. at the $z = i\Delta z$, the scaling $E_x$ coefficient for the $i - cell$ has to be set to zero for each time-step $m$. Nevertheless, the 0-resolution wavelet for the same cell has an inherent value of zero at its midpoint; thus its amplitude does not have to be set to zero. The enforcement of the physical requirement that the electric field values on either side of the conductor are independent from the values on the other side, TWO 0-resolution wavelet $E_x$ coefficients have to be defined, one for each side of the P.E.C. Wavelet coefficients of higher-resolution with domains tangential to the position of P.E.C. have to be zeroed out as well.

Starting from the constitutive relationship $D_x = \epsilon E_x$ for the total electric field at one mesh point and sampling the scaling components with a similar way to [1], the dielectric interfaces can be modeled through a system of equations similar to the following describing the scaling coeficient

$$
{}_mD^{\phi}_{x,i} = d^{\phi}_{\phi d}(i)\, {}_mE^{\phi}_{x,i} + \sum_{r=0}^{r_{max}} \sum_{i_r=1}^{2^r} d^{\psi_r,i_r}_{\phi d}(i)\ {}_mE^{\psi_r,i_r}_{x,i} \quad (3)
$$

where

$$
\left\{ \begin{array}{c} d^{\phi}_{\phi d}(i) \\ d^{\psi_r,i_r}_{\phi d}(i) \end{array} \right\} = \int_{(i-0.5)\Delta z}^{(i+0.5)\Delta z} \epsilon(z)\ \phi_i(z) \left\{ \begin{array}{c} \phi_i(z) \\ \psi_i^{r,i_r}(z) \end{array} \right\} dz
$$

The system of equations can be written compactly

$$
[\bar{D}_x] = [\bar{\bar{\epsilon}}][\bar{E}_x] \quad . \quad (4)
$$

Due to the orthogonality relationhip between the scaling/wavelet functions, for uniform dielectrics (constant $\epsilon$ throughout the integration domain), $[\bar{\bar{\epsilon}}]$ becomes a diagonal matrix. For structures containing dielectric discontinuities, none of these integrals have a zero value. In this case, the whole geometry has to be preprocessed before the initialization of the time loop and coefficients $d$ have to be assigned to any $i - cell$ and included in the matrix $[\bar{\bar{\epsilon}}]$. This matrix can be sparsified by zeroing-out all coefficients that are below a relative threshold of the diagonal term(usually $\leq 0.1\%$) of each raw. This new matrix has significantly larger sparsity and contains only cells close to dielectric discontinuities. The inverse of this matrix is used for the calculation of the E from the D values for each time step. This inversion takes place only once, thus it adds only negligible computational overhead to the algorithm. The procedure can be extended to more than 1 dimensions using double and triple integrals for the calculation of $d$. Since these integrals are independent of the number and the direction of the intracell dielectric interfaces, this technique can be used for any dielectric configuration.

# III MRTD Modeling of Si-Micromachined FG-CPW's

Micromachined FG-CPW lines have a geometry similar to conventional FG-CPW lines, except that the material underneath the line apertures has been removed creating grooves (Fig.(2)). The resulting micromachined line has all the advantages of conventional CPW, but the width of the line and the depth of the grooves provide direct control over the effective dielectric constant $\epsilon_{eff}$ and the loss. The modeled Finite-Ground Coplanar Waveguide [7] has a center conductor width s=40$\mu$m, signal-to-ground distance $w = 80\mu m$ and has been fabricated on $500\mu m$ thick Si substrate, deriving a cutoff frequency of the first higher order mode of 120GHz. The backside of the wafer is not metallized. The < 111 > etching direction creates a nonorthogonal air-dielectric interface, that sets a challenge for the conventional time-domain techniques. For the analysis of the structure, a 2.5D MRTD mesh of $30 \times 50$ with a cell size equal to $20 \times 50\mu m$ is used for propagation constant $\beta = 20$. The threshold values for the wavelet memory compression are $10^{-6}$ (Absolute) and $10^{-4}$ (Relative) and offer additional memory compression by a 95% for used wavelets up to the 4th resolution ($r_{max}$=4) for both directions of the dielectric undercut plane (Max:1800 coefs). Higher resolution wavelets can be added, but results show only minimal improvement in terms of accuracy. The same structure has been also analyzed, for comparison, with FDTD method using a coarse grid with cell size equal to the MRTD grid (C-FDTD with 1500 cells) and a dense grid that uses 4 times smaller cell (D-FDTD with 24000 cells). The structure has been excited using Gaussian line excitation between the signal and the ground planes with frequency content [0,100GHz] and odd spatial symmetry, in order to excite only the CPW mode and PML absorber terminates the grid. Though FDTD simulation has required the staircase approximation of the nonorthogonal dielectric interface, MRTD uses grid cells containing both air and dielectric substrate by using the equations (3),(4) extended in 2D. In addition, due to the fact that the wavelets have significant values only close to the undercut interfaces, the additional memory overhead is much smaller than the factor $4^2$, that is required by FDTD dense grid.

Table (1) shows the good agreement of MRTD and dense FDTD with the measurements for the $Z_o$ for undercuts (UC) $0 - 10\mu m$ at f=94 GHz. The results obtained by coarse FDTD have an absolute maximum error larger than 7.8%. Figs. (3),(4) show the variation of $\epsilon_{eff}$ as a function of the size of the dielectric undercut and of the frequency range. Though the decrease of $\epsilon_{eff}$ is sharp for small values of undercut, it converges to the microshield value for undercuts approximately larger than $28\mu m$. This decreasing trend is the major reason for a decreasing attenuation and increasing characteristic impedance. In addition, the almost constant behavior of $\epsilon_{eff}$ with frequency confirms the assumption for a single-mode TEM propagation. Thus, no viaholes are needed, resulting in single-side wafer processing.

**Table 1: $Z_o$ ($\Omega$) at f=94GHz**

| UC($\mu m$) | 0 | 2 | 6 | 10 | $\|Max.Err.\|$ |
|---|---|---|---|---|---|
| Meas[7] | 64 | 70.2 | 80.8 | 87.6 | (-) |
| MRTD | 64.4 | 70.7 | 81.2 | 88.3 | (0.8%) |
| FDTD-C | 60.2 | 65.4 | 75.2 | 80.8 | (7.8%) |
| FDTD-D | 63.5 | 69.6 | 80.3 | 87.0 | (0.9%) |

# IV Conclusion

An efficient algorithm for the modeling of micromachined transmission lines with the MRTD scheme based on Haar basis has been proposed and has been applied to the numerical analysis of Si-micromachined FG-CPW's. The effective dielectric constant has been calculated and verified by comparison to reference data for various dielectric undercuts and frequencies. In comparison to Yee's conventional FDTD scheme, the proposed scheme offers memory savings by a factor of 2-8 per dimension maintaining a similar accuracy without any approximations.

# V Acknowledgments

This work has been supported by GT-Packaging Research Center and by the Yamacraw initiative.

## References

[1] M.Krumpholz, L.P.B.Katehi, "MRTD: New Time Domain Schemes Based on Multiresolution Analysis", IEEE Trans. Microwave Theory Tech., pp. 555-572, 1996.

[2] E.Tentzeris, R.Robertson, A.Cangellaris, L.P.B.Katehi, "Space- and Time-Adaptive Gridding Using MRTD", Proc. MTT-S 1997, pp. 337-340.

[3] R.L.Robertson. E.Tentzeris and L.P.B.Katehi, "Modelling of Dielectric-Loaded Cavities using MRTD", Int. Journal of Numerical Modeling, Special Issue on Wavelets in Electromagnetics, Vol.11, pp.55-68, 1998.

[4] K.Goverdhanam, E.Tentzeris, M.Krumpholz and L.P.B. Katehi, "An FDTD Multigrid based on Multiresolution Analysis", Proc. AP-S 1996, pp. 352-355.

[5] M.Fujii, W.J.R.Hoefer, "Formulation of a Haar-wavelet based Multiresolution Analysis similar to the 3-D FDTD Method", Proc. MTT-S 1998, pp. 1393-1396.

[6] C.Sarris and L.P.B.Katehi, "Multiresolution Time Domain (MRTD) Schemes with Space-Time Haar Wavelets", Proc. MTT-S 1999, pp. 1459-1462.

[7] K.Herrick, T.Schwarz, L.P.B.Katehi, "Si-Micromachined Coplanar Waveguides for Use in High-Frequency Circuits", IEEE Trans. MTT, pp. 762-768, June 1998.

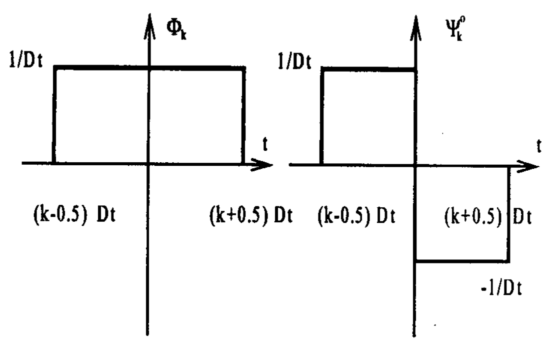


Figure 1: Haar Expansion Basis.

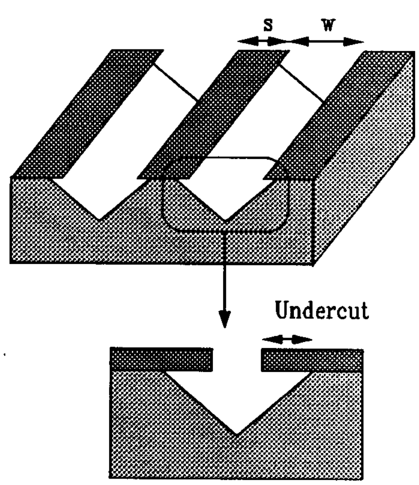


Figure 2: Si-micromachined FG-CPW.

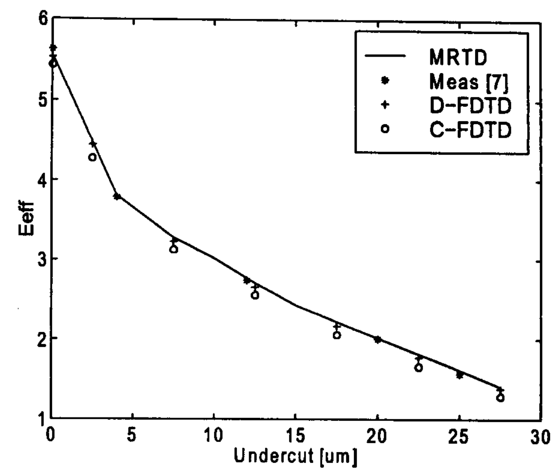


Figure 3: Effective Dielectric Constant as a function of Undercut.

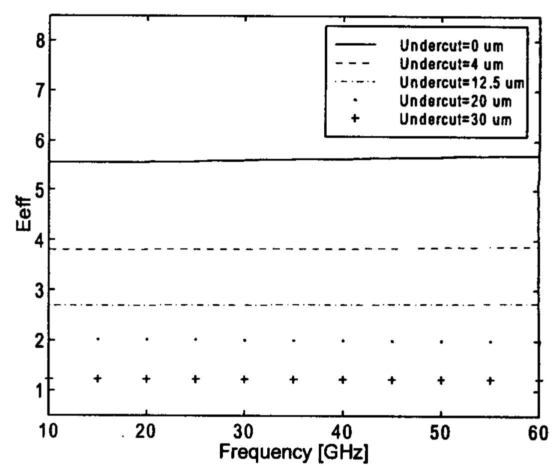


Figure 4: Effective Dielectric Constant as a function of Frequency.